



Tang, Qi, Zheng, Meng, Sheng, Yanqing and Mortimer, Robert  
ORCID logo ORCID: <https://orcid.org/0000-0003-1292-8861> (2019)  
Simultaneous nitrification and denitrification using a novel up-flow  
bio-electrochemical reactor. *Desalination and Water Treatment*,  
158. pp. 97-104.

Downloaded from: <https://ray.yorks.ac.uk/id/eprint/4888/>

The version presented here may differ from the published version or version of record. If  
you intend to cite from the work you are advised to consult the publisher's version:

[https://www.deswater.com/DWT\\_abstracts/vol\\_158/158\\_2019\\_97.pdf](https://www.deswater.com/DWT_abstracts/vol_158/158_2019_97.pdf)

Research at York St John (RaY) is an institutional repository. It supports the principles of  
open access by making the research outputs of the University available in digital form.  
Copyright of the items stored in RaY reside with the authors and/or other copyright  
owners. Users may access full text items free of charge, and may download a copy for  
private study or non-commercial research. For further reuse terms, see licence terms  
governing individual outputs. [Institutional Repositories Policy Statement](#)

# RaY

Research at the University of York St John

For more information please contact RaY at  
[ray@yorks.ac.uk](mailto:ray@yorks.ac.uk)

**Simultaneous nitrification and denitrification using a novel up-flow  
bio-electrochemical reactor**

Qi Tang<sup>1,2</sup>, Meng Zheng<sup>1</sup>, Yanqing Sheng<sup>1,\*</sup> and Robert J.G. Mortimer<sup>3</sup>

1 Research Center for Coastal Environment Engineering Technology of Shandong Province,  
Yantai Institute of Coastal Zone Research, Chinese Academy of Sciences, Yantai 264003, China

2 University of Chinese Academy of Sciences, Beijing, China

3 School of Animal, Rural and Environmental Sciences, Nottingham Trent University,  
Brackenhurst campus, Southwell, Nottinghamshire. NG25 0QF, UK

\* Corresponding author; E-Mail: [yqsheng@yic.ac.cn](mailto:yqsheng@yic.ac.cn) Tel.: +86-535-210-9265; Fax:  
+86-535-210-9000.

Qi Tang, E-Mail: [qtang@yic.ac.cn](mailto:qtang@yic.ac.cn);

Meng Zheng, E-Mail: [mzheng@yic.ac.cn](mailto:mzheng@yic.ac.cn);

Robert J.G. Mortimer, E-Mail: [Robert.Mortimer@ntu.ac.uk](mailto:Robert.Mortimer@ntu.ac.uk)

**Abstract:**

Nitrogen removal is a problem in the field of water treatment, especially in the presence of sulfate. Conventional nitrification and denitrification are usually carried out in two separate reactors. In addition, the effect of sulfate on hydrogenotrophic denitrification is not clear. In this study, simultaneous nitrification and denitrification (SND) for nitrogen removal from water was conducted using a single novel up-flow bio-electrochemical reactor (UBER). The influence of dissolved oxygen (DO) on nitrogen removal was investigated. When influent DO was 7.0 – 8.0 mg L<sup>-1</sup>, a heterotrophic nitrification zone (with DO 3.2 – 5.5 mg L<sup>-1</sup>) and a hydrogenotrophic denitrification zone (with DO 1.6 – 4.2 mg L<sup>-1</sup>) were obtained within the reactor, and the removal rates of NH<sub>4</sub><sup>+</sup>-N and TN reached more than 90%. The distribution of DO

inside developing biofilms was measured using microelectrodes. When DO in the hydrogenotrophic denitrification zone was  $2.9 \text{ mg L}^{-1}$ , DO inside the biofilm was just  $0.5 \text{ mg L}^{-1}$ . The effect of sulfate on hydrogenotrophic denitrification was studied by regulating the S/N ratio of influent water. Simultaneous removal of nitrate and sulfate can be achieved at low S/N, and the removal rates of nitrate and sulfate were ~80%. With increasing S/N ratio, sulfide produced by sulfate reduction inhibited both denitrification and further sulfate reduction.

**Keywords:** Nitrification and denitrification; Bio-electrochemical reactor; Biofilm; Sulfate

## 1. Introduction

Nitrogenous contaminants such as nitrate and ammonia can promote eutrophication, causing deterioration of water quality and posing potential hazards to human or animal health [1]. Therefore, different technologies such as reverse osmosis, chemical denitrification and biological denitrification have been developed to remove nitrogenous contaminants from water bodies [2]. Simultaneous nitrification and denitrification (SND) is one of the most widely accepted biological solutions for removing nitrogen from high ionic strength nitrogenous wastewaters [3]. SND is highly effective at removing nitrogen compounds [4-5] because it uses small reaction volumes, has short reaction times and low energy consumption [6-7]. It is estimated that the SND process utilizes 22-40% less carbon and reduces sludge yield by 30%

compared with conventional nitrification and denitrification systems [8]. Through the SND process, oxygen and  $\text{NO}_3^-$ -N can fully be utilized as the alternate electron acceptors, which results in low DO [9-10]. Additionally, SND can be accomplished at neutral pH because it is self-buffering, with alkalinity produced during denitrification consumed during nitrification. Robertson *et al.* [11] reported that the experimental conditions for SND were difficult to control in one reactor. Consequently, it is necessary to develop a novel reactor for SND to ensure different microbial communities are distributed effectively, and don't change with changing influent load.

The “bio-electrochemical reactor” system is a novel method for water and wastewater denitrification that improves biological denitrification by immobilizing autohydrogenotrophic bacteria directly on the surface of a cathode to provide easy access to  $\text{NO}_3^-$  and  $\text{H}_2$  as the electron acceptor and electron donor respectively [12]. Eq. (1) shows the general reaction leading to autohydrogenotrophic denitrification in aqueous solution. Ghafari *et al.* [13] demonstrated co-existence of both aerobic and anoxic zones in a single up-flow bio-electrochemical reactor (UBER), which had a high chemical oxygen demand (COD) and efficient nitrogen removal.



Another limiting factor on N removal treatment systems is sulfate, which is common in natural water bodies and wastewaters. Under anaerobic or anoxic conditions, nitrate and sulfate can be reduced to nitrogen and sulfide by denitrifying bacteria and sulfate reducing bacteria, respectively. Nitrate reduction is

thermodynamically more favourable than sulfate reduction [14]. Chen *et al.* [15] found that the degree of  $\text{SO}_4^{2-}$  reduction steadily decreased with higher influent  $\text{NO}_3^-$  concentration. Conversely, the end product of sulfate reduction, sulfide, is harmful to microorganisms at high concentration and has the potential to both inhibit N removal processes and prevent further sulfate reduction. The relationship between nitrate and sulfate in low DO environments therefore needs further study.

The goal of this study was (1) to design a novel reactor which combined heterotrophic nitrification and hydrogenotrophic denitrification for SND (2) to investigate nitrogen removal efficiency and DO distribution in biofilms in the reactor (3) to explore the effect of sulfate on hydrogenotrophic denitrification.

## **2. Materials and methods**

### **2.1. Experimental apparatus**

A schematic of the lab-scale novel UBER used in the study is shown in Fig. 1. The new UBER for SND was divided into two functional units, a lower heterotrophic nitrification zone and an upper hydrogenotrophic denitrification zone, to ensure different microbial communities were distributed effectively. The apparatus for experiments on the effect of sulfate has the same volume and arrangement of experimental materials but without the heterotrophic nitrification zone.

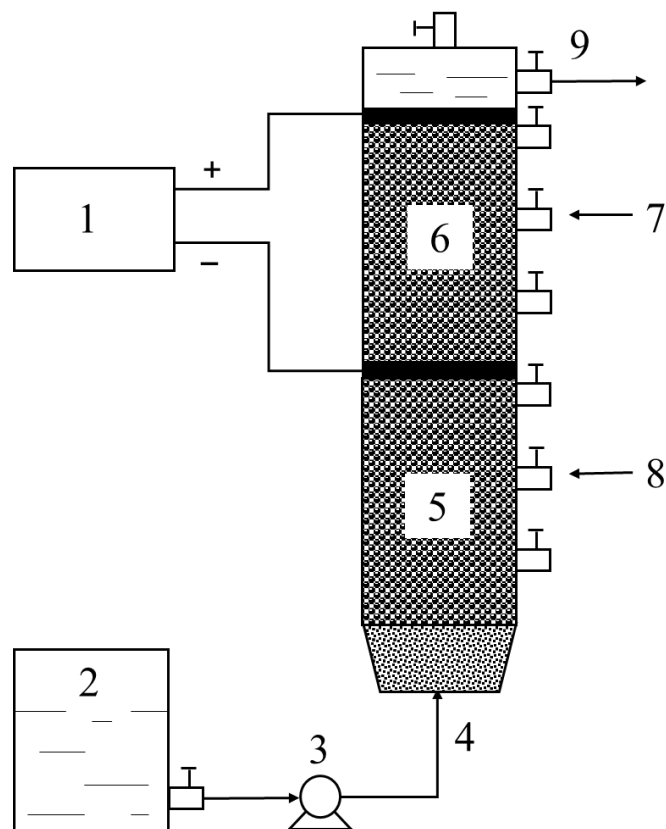


Fig. 1 Schematic of UBER for SND. (1) DC power supply; (2) influent tank; (3) influent pump; (4) inlet; (5) heterotrophic nitrification zone; (6) hydrogenotrophic denitrification zone; (7) sampling tap 1; (8) sampling tap 2; (9) outlet

The UBER was built using a 2 L Plexiglass cylindrical column (inside diameter of 9.2 cm, height 35cm), sealed at the top. A stainless steel wire mesh was installed at the middle of the reactor as a cathode and a carbon rod (8.8 cm long) was installed at the top of the reactor as the anode. An adjustable power supply (APS3005D, Shenzhen, China) was applied to provide direct current. One inlet port was installed at the bottom of the cylindrical column, and one outlet port was installed 27 cm from the bottom, leaving a 3 cm head space. Sampling points were installed every 5 cm from the bottom. Sampling tap 1 and tap 2 were installed 25 cm and 10 cm from the bottom,

respectively. The reactor was filled with carbon granules (in size range of 1-2 cm) which were washed with deionized water four times prior to use. To provide a sticky surface for microorganisms on the carbon granules, they were saturated and boiled in 2% agar solution. The total volume of carbon granules was 1 L, accounting for 50% of the reactor's capacity. The reactor was covered with aluminium foil to exclude light and prevent algal growth.

## **2.2. Synthetic influent and sludge**

Based on the water quality that is characteristic of local polluted rivers, reservoirs and groundwater [16], synthetic wastewater for this work was prepared with a low C/N ratio. The composition of synthetic wastewater for the SND experiments comprised; glucose ( $0.6 \text{ g L}^{-1}$ ),  $\text{NH}_4\text{Cl}$  ( $0.23 \text{ g L}^{-1}$ ),  $\text{KH}_2\text{PO}_4$  ( $0.013 \text{ g L}^{-1}$ ),  $\text{MgSO}_4 \cdot 7\text{H}_2\text{O}$  ( $0.02 \text{ g L}^{-1}$ ),  $\text{CaCl}_2 \cdot 2\text{H}_2\text{O}$  ( $0.001 \text{ g L}^{-1}$ ),  $\text{FeSO}_4 \cdot 7\text{H}_2\text{O}$  ( $0.001 \text{ g L}^{-1}$ ),  $\text{NaHCO}_3$  ( $0.252 \text{ g L}^{-1}$ ) and 1 ml trace solution. The components of the trace solution were  $\text{ZnSO}_4 \cdot 7\text{H}_2\text{O}$  ( $100 \text{ mg L}^{-1}$ ),  $\text{MnCl}_2 \cdot 4\text{H}_2\text{O}$  ( $30 \text{ mg L}^{-1}$ ),  $\text{H}_3\text{BO}_3$  ( $300 \text{ mg L}^{-1}$ ),  $\text{CoCl}_2 \cdot 6\text{H}_2\text{O}$  ( $200 \text{ mg L}^{-1}$ ),  $\text{CuCl}_2 \cdot 2\text{H}_2\text{O}$  ( $10 \text{ mg L}^{-1}$ ),  $\text{NiCl}_2 \cdot 2\text{H}_2\text{O}$  ( $10 \text{ mg L}^{-1}$ ),  $\text{Na}_2\text{MoO}_4 \cdot 2\text{H}_2\text{O}$  ( $30 \text{ mg L}^{-1}$ ) and  $\text{Na}_2\text{SeO}_3$  ( $30 \text{ mg L}^{-1}$ ). Oxygen ( $\text{O}_2$ ) was added from a gas cylinder to adjust the DO of the influent on demand. Aerobic and anaerobic sludge were obtained from a secondary sedimentation tank and an anaerobic digester tank in the Xin'anhe Municipal Wastewater Treatment Plant in Yantai, China. Aerobic and anaerobic sludge were aerated with oxygen and bubbled with nitrogen, respectively, for 24 h. The two kinds of activated sludge were mixed in equal volumes

prior to pouring (1 L) into the reactor.

The simulated wastewater composition for the sulfate effect experiments comprised:  $\text{NaHCO}_3$  ( $0.252 \text{ g L}^{-1}$ ),  $\text{MgSO}_4 \cdot 7\text{H}_2\text{O}$  ( $0.34 \text{ g L}^{-1}$ ),  $\text{FeCl}_3$  ( $0.1 \text{ g L}^{-1}$ ),  $\text{KH}_2\text{PO}_4$  ( $0.027 \text{ g L}^{-1}$ ),  $\text{CaCl}_2$  ( $0.3 \text{ g L}^{-1}$ ), 1 ml trace solution I and 1 ml trace solution II. The components in trace solution I were:  $\text{EDTA}$  ( $5 \text{ g L}^{-1}$ ),  $\text{FeSO}_4$  ( $5 \text{ g L}^{-1}$ ). The components in trace solution II were:  $\text{EDTA}$  ( $15 \text{ g L}^{-1}$ ),  $\text{H}_3\text{BO}_3$  ( $0.014 \text{ g L}^{-1}$ ),  $\text{MnCl}_2 \cdot 4\text{H}_2\text{O}$  ( $0.99 \text{ g L}^{-1}$ ),  $\text{CuSO}_4 \cdot 5\text{H}_2\text{O}$  ( $0.25 \text{ g L}^{-1}$ ),  $\text{CoCl}_2 \cdot 6\text{H}_2\text{O}$  ( $0.24 \text{ g L}^{-1}$ ),  $\text{ZnSO}_4 \cdot 7\text{H}_2\text{O}$  ( $0.43 \text{ g L}^{-1}$ ),  $\text{NiCl}_2 \cdot 6\text{H}_2\text{O}$  ( $0.19 \text{ g L}^{-1}$ ),  $\text{Na}_2\text{MoO}_4 \cdot 2\text{H}_2\text{O}$  ( $0.22 \text{ g L}^{-1}$ ) and  $\text{Na}_2\text{SeO}_3 \cdot 10\text{H}_2\text{O}$  ( $0.21 \text{ g L}^{-1}$ ). The concentrations of  $\text{NaNO}_3$  and  $\text{Na}_2\text{SO}_4$  were added as required for the experiment. The simulated wastewater was purged with nitrogen for 1 h to remove residual oxygen. Anaerobic sludge was bubbled with nitrogen for 24 h before pouring (1 L) into the reactor.

### **2.3. Experimental conditions**

The removal rates of  $\text{NH}_4^+\text{-N}$  and total nitrogen (TN) in the reactor were investigated under different conditions. At the beginning of the experiment, the pH of the synthetic wastewater was adjusted to 7.5 using  $\text{NaHCO}_3$ . The temperature was controlled at  $30 \pm 2^\circ\text{C}$  to accelerate the reaction rate and shorten the experimental period. The bio-electrochemical reactor was operated with a feed of 200 ml/h synthetic wastewater (hydraulic retention time = 10 h). DO concentration in the bulk solution inside the reactor was set by adjusting inflow at different phases. The UBER experiment lasted 95 days and was divided into 4 phases: days 1-30, 31-50,



51-70 and 71-95 (Table 1). These phase divisions ensured that the biofilm had enough time to mature and stabilize. In phase 1, the influent DO was adjusted to 5 mg L<sup>-1</sup>. Consequently, the influent DO was adjusted to 6 mg L<sup>-1</sup> in phase 2, 7 mg L<sup>-1</sup> in phase 3, and to 8 mg L<sup>-1</sup> in phase 4 (Table 1).

The effect of sulfate on hydrogenotrophic denitrification performance in the reactor was studied by regulating the influent S/N. Three experiments were conducted with S/N ratios of 1:2 (SO<sub>4</sub><sup>2-</sup>-S: 25mg L<sup>-1</sup>, NO<sub>3</sub><sup>-</sup>-N: 50mg L<sup>-1</sup>), 1:1(SO<sub>4</sub><sup>2-</sup>-S: 50mg L<sup>-1</sup>, NO<sub>3</sub><sup>-</sup>-N: 50mg L<sup>-1</sup>) and 2:1 (SO<sub>4</sub><sup>2-</sup>-S: 50mg L<sup>-1</sup>, NO<sub>3</sub><sup>-</sup>-N: 25mg L<sup>-1</sup>) respectively. The experiments were carried out at 30 ± 2°C, 10 mA electric current and 6 hours of hydraulic retention time until the effluent parameters were stable.

Table 1 Detailed operating conditions

	Phase1	Phase 2	Phase 3	Phase 4
Operation period (day)	30	20	20	25
Hydraulic retention time (h)	10	10	10	10
Electric current (mA)	20	20	20	20
Influent DO (mg L <sup>-1</sup> )	5	6	7	8
T (°C)	30	30	30	30
Influent NH <sub>4</sub> <sup>+</sup> -N (mg L <sup>-1</sup> )	60	60	60	60

#### 2.4. Sampling and analysis

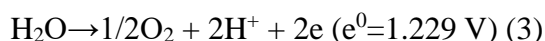
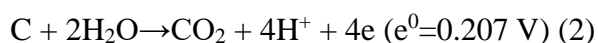
Samples were collected from the sampling taps. The pH, temperature (T) and DO were measured immediately using a pH meter (PSH-3C, China), thermometer, and oxygen microelectrode (PRO 3.0, Unisense, Denmark). The COD of the effluent was measured using the potassium dichromate method. Then, remaining water samples

were filtered using 0.2 $\mu$ m syringe filters prior to analysis for NH<sub>4</sub><sup>+</sup>-N, NO<sub>3</sub><sup>-</sup>-N, and NO<sub>2</sub><sup>-</sup>-N using an Autoanalyzer III (Seal, Germany) with an analytical precision of 0.5‰ unit. SO<sub>4</sub><sup>2-</sup>-S and sulfide were analyzed by an ion chromatograph (Dionex ICS3000, USA) and iodometric titration method [17] respectively. TN was detected using an UV spectrophotometry meter (TU-1950, Persee, Beijing, China). The DO distribution in the biofilm (adhered to the carbon granule surface) with depth was measured using a miniaturized Clark-type oxygen sensor with a guard cathode (DO microsensor, Unisense Microsensor, Denmark). A Micro Profiling System (Unisense) was used to control the penetration distance and acquire data.

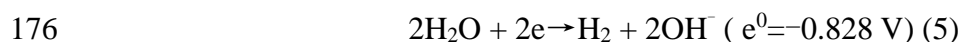
### 3. Results and discussion

#### 3.1. Start-up of the novel UBER

DO level, electric current and hydraulic retention time are three important factors in the nitrification and denitrification process. In this study, the novel UBER was operated for 95 days (phases 1-4) with different influent DO values (Table 1). During phase1, high current (20 mA), high temperature (30°C), short hydraulic retention time (10 h) and 5.0 mg L<sup>-1</sup> DO were applied to supply sufficient substrates to support microbial activity (inoculated aerobic sludge and anaerobic sludge). The possible electrochemical reactions at the anode include:



And the possible electrochemical reactions at the cathode are



177 According to reaction (2) and (3),  $\text{CO}_2$  is formed prior to  $\text{O}_2$  at the anode. This  $\text{CO}_2$   
 178 could serve as pH buffer and inorganic carbon source. The hydrogen gas produced  
 179 from the cathode serves as the electron donor for hydrogenotrophic denitrification.

180 Fig. 2 shows the variations in water quality between the lower and upper zone. In  
 181 the first two days, the effluent concentration of  $\text{NH}_4^+\text{-N}$  was a little higher than initial  
 182 influent concentration ( $60 \text{ mg L}^{-1}$ ), which may be due to the death of bacteria which  
 183 cannot adapt to the influent conditions. In the lower zone,  $\text{NH}_4^+\text{-N}$  and COD declined  
 184 sharply while  $\text{NO}_3^-\text{-N}$  increased gradually and remained stable during the whole  
 185 period. During phase 4, the steady concentrations of  $\text{NH}_4^+\text{-N}$ ,  $\text{NO}_2^-\text{-N}$  and  $\text{NO}_3^-\text{-N}$   
 186 were  $3.5 \text{ mg L}^{-1}$ ,  $1.5 \text{ mg L}^{-1}$  and  $24.1 \text{ mg L}^{-1}$ , respectively. There were  $\sim 56.5 \text{ mg L}^{-1} \text{ N}$   
 187 removed as  $\text{NH}_4^+\text{-N}$  and  $25.6 \text{ mg L}^{-1} \text{ N}$  produced as  $\text{NO}_2^-\text{-N}$  and  $\text{NO}_3^-\text{-N}$ . The  
 188 removal rate of  $\text{NH}_4^+\text{-N}$  reached 96.5% at the end of phase 4 (Fig. 2c). These results  
 189 indicate that nitrification occurred in the lower zone. This may include a variety of  
 190 nitrification reactions, such as heterotrophic nitrification and autotrophic nitrification.  
 191 In contrast chemoautotrophic nitrifiers, heterotrophic nitrifiers can use both inorganic  
 192 and organic substrates for nitrification [18-19]. A high C/N ratio can stimulate the  
 193 growth of heterotrophic bacteria and inhibit the activity of autotrophic nitrifiers [20].  
 194 In the presence of large amounts of organic matter, autotrophic nitrifying bacteria  
 195 have less competition for oxygen and organic matter than aerobic heterotrophic

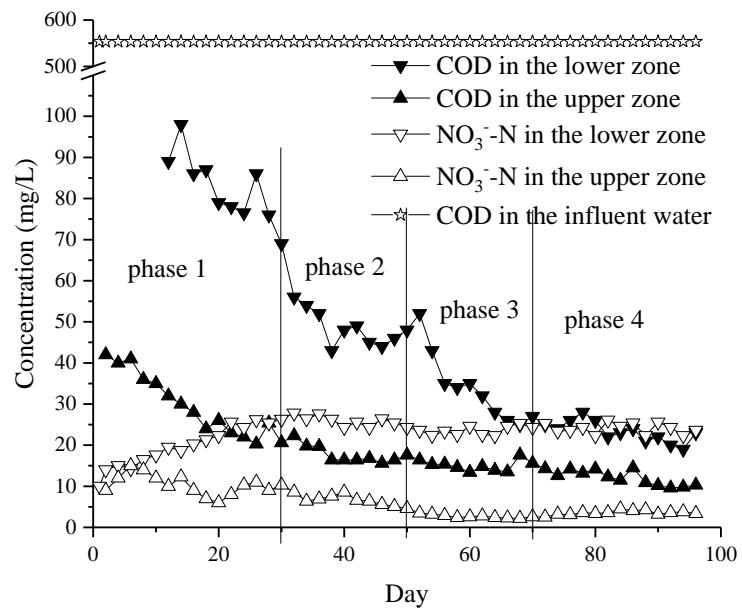
bacteria, allowing the heterotrophs to become predominant.

In the upper zone effluent water, there was no significant variations in  $\text{NH}_4^+\text{-N}$  and  $\text{NO}_2^-\text{-N}$  between the upper zone effluent and the lower zone effluent, but the concentration of  $\text{NO}_3^-\text{-N}$  showed a distinct decline. This implied that denitrification mainly occurred in the upper zone. Both  $\text{H}_2$  and organic matter can be used as electron donor for denitrification in the reactor. The maximum denitrification rate in the upper zone was  $0.055 \text{ kg NO}_3^-\text{-N}/(\text{m}^3 \text{ d})$ , and it was close to the similar bio-electrochemical denitrification reactor, indicating that hydrogenotrophic denitrification dominated in the upper zone.

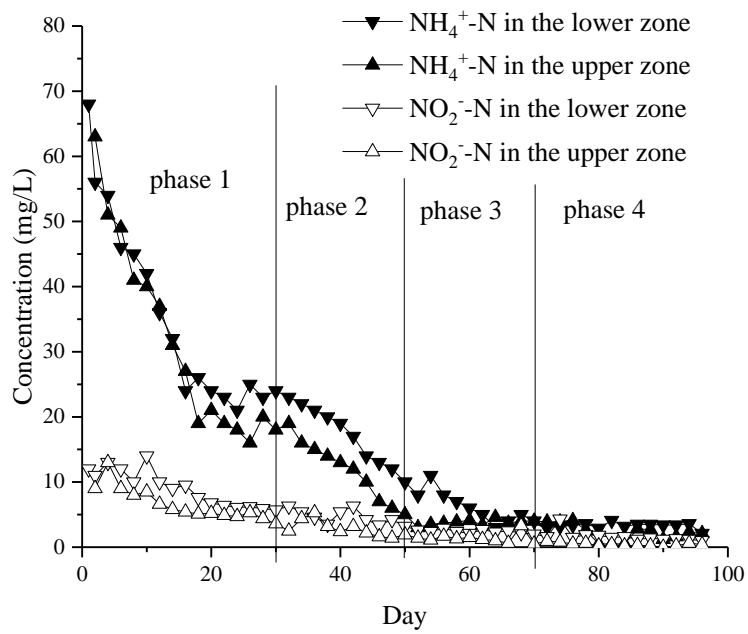
In general, the hydrogenotrophic denitrification occurs at lower rates than heterotrophic denitrification owing to slower bacterial growth rates [2]. For example, Hamlin *et al.* used four kinds of organics as carbon sources and the obtained maximum daily denitrification rate was  $0.67\text{--}0.68 \text{ kg NO}_3^-\text{-N}/(\text{m}^3 \text{ d})$ , regardless of the carbon source [21]. The average denitrification rate was  $0.62 \text{ kg NO}_3^-\text{-N}/(\text{m}^3 \text{ d})$  in the ethanol supported system [22]. Sunger and Bose [23] achieved a denitrification rate of  $0.027 \text{ kg NO}_3^-\text{-N}/(\text{m}^3 \text{ d})$  in a fixed-bed hydrogenotrophic denitrification system. Park *et al.* [24] achieved a higher denitrification rate ( $0.077\text{--}1.68 \text{ kg NO}_3^-\text{-N}/(\text{m}^3 \text{ d})$ ) using a bio-electrochemical reactor.

After 30 days, concentrations of  $\text{NH}_4^+\text{-N}$ ,  $\text{NO}_3^-\text{-N}$ , and COD in the upper zone effluent reached  $19.2 \text{ mg L}^{-1}$ ,  $8.6 \text{ mg L}^{-1}$ , and  $22.3 \text{ mg L}^{-1}$ , respectively (Fig. 2). Generally, stable water quality of the outlet and the color of biofilm can be used as

indicators of the mature status of the biofilm. In this study, stable water quality and dark brown biofilm on the carriers (carbon granules) showed that the microbiological UBER systems had established after 30 days. In the lower zone,  $\text{NO}_3^-$ -N increased to 26.3  $\text{mg L}^{-1}$  at the end of phase 1 and remained at similar levels from phase 2 to phase 4. Meanwhile,  $\text{NH}_4^+$ -N decreased to  $\sim 3 \text{ mg L}^{-1}$  from phase 2 to phase 4, and the removal rate of COD reached 95.8% at the end of phase 4. In the upper zone, after phase 2, both of  $\text{NO}_3^-$ -N and  $\text{NO}_2^-$ -N were  $< 5 \text{ mg L}^{-1}$ , and  $\text{NH}_4^+$ -N and COD kept low levels ( $\sim 5 \text{ mg L}^{-1}$  and  $\sim 15 \text{ mg L}^{-1}$ , respectively). These results demonstrate that heterotrophic nitrification and hydrogenotrophic denitrification was stable in the lower and upper zone respectively. As shown in Fig. 2(c), microbes maintained the ability to remove organic matter with more than 90% COD removal rate during the process of inoculation and acclimation (phase1). In the last phase, the removal rate of COD was up to 98%. The COD removal efficiency of the bio-electrochemical reactor was excellent.



(a)



(b)

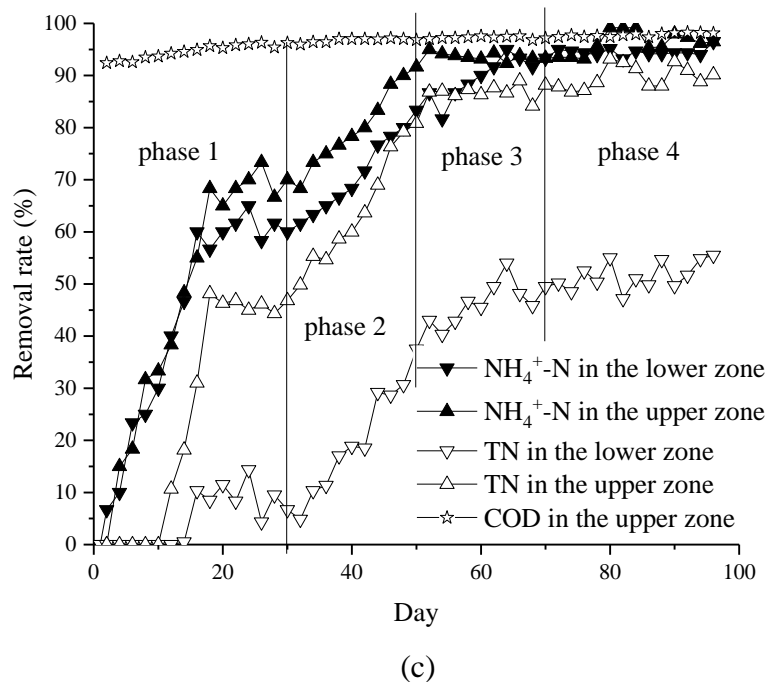


Fig. 2 Profiles of COD and  $\text{NO}_3^-$ -N (a),  $\text{NH}_4^+$ -N and  $\text{NO}_2^-$ -N (b), and  $\text{NH}_4^+$ -N and TN removal rate (c) over time

### 3.2. Influence of DO on the nitrogen removal

During the experimental process, influent DO levels in influents were adjusted to 5, 6, 7 and 8  $\text{mg L}^{-1}$  in phases 1, 2, 3 and 4, respectively. The relationship between DO and nitrogen removal is shown in Fig. 2 and Fig. 3. As shown in the lower heterotrophic nitrification section, the  $\text{NH}_4^+$ -N and TN removal rates in phase 2 were 83.3% and 37.5%, respectively, with 3.2  $\text{mg L}^{-1}$  DO. In phase 3, DO increased to 4.8  $\text{mg L}^{-1}$ , and the removal rates of  $\text{NH}_4^+$ -N and TN gradually increased to 93.3% and 49.5%, respectively (Fig. 2c). In the upper hydrogenotrophic denitrification section, the removal rates of  $\text{NH}_4^+$ -N and TN reached 80% while the DO level was 1.7  $\text{mg L}^{-1}$  at phase 2. In phase 3,  $\text{NH}_4^+$ -N and TN removal rates achieved 90% with 2.4  $\text{mg L}^{-1}$  DO level (Fig. 2c).

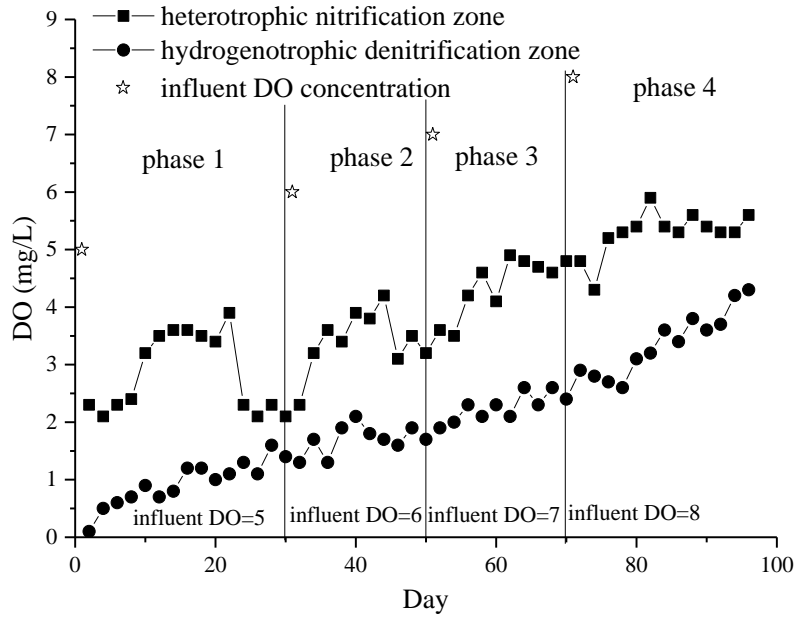


Fig. 3 Variations of DO in the heterotrophic nitrification zone and hydrogenotrophic denitrification zone

In phase 4, the DO levels in bulk solution increased further to  $5.5 \text{ mg L}^{-1}$  and  $4.2 \text{ mg L}^{-1}$  in the heterotrophic nitrification and hydrogenotrophic denitrification zones, respectively, by increasing influent DO levels to  $8.0 \text{ mg L}^{-1}$ . At this stage, the effluent quality parameters such as  $\text{NH}_4^+\text{-N}$  and  $\text{NO}_2^-\text{-N}$  remained stable (Fig. 2). Meanwhile, the TN removal rates of the reactor were kept stable (above 90%). This phenomenon indicated that the hydrogenotrophic denitrification was not restricted by relatively high DO level ( $4.2 \text{ mg L}^{-1}$ ). Deng *et al.* [25] had similar results, showing that the autotrophic denitrification process using hydrogen from Fe–C galvanic cells as an electron donor was not affected by DO. Li *et al.* [26] also had similar findings, with maximum nitrogen removal efficiency of 96.5% while the DO concentrations of influent and effluent were  $7.95$  and  $6.74 \text{ mg L}^{-1}$ , respectively. As shown in Fig. 3, DO levels were well below the influent levels throughout. The decline of DO



concentrations (about  $1.3 \text{ mg L}^{-1}$ ) in the hydrogenotrophic denitrification zone between influent and effluent was likely due to consumption by aerobic denitrifiers [27]. The microbial community in the reactor needs to be studied.

### 3.3. Simultaneous nitrification and denitrification

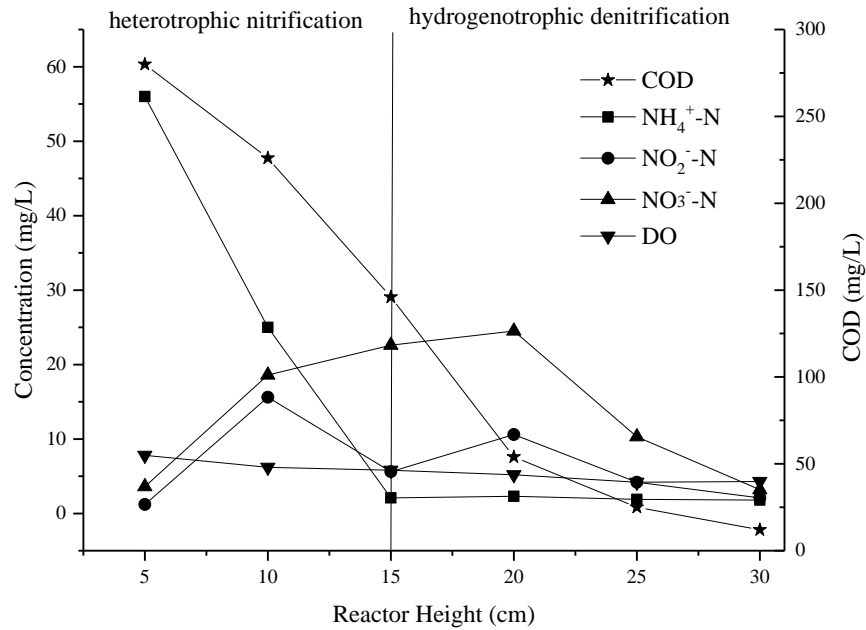


Fig. 4 The water quality parameters at different depths of the reactor

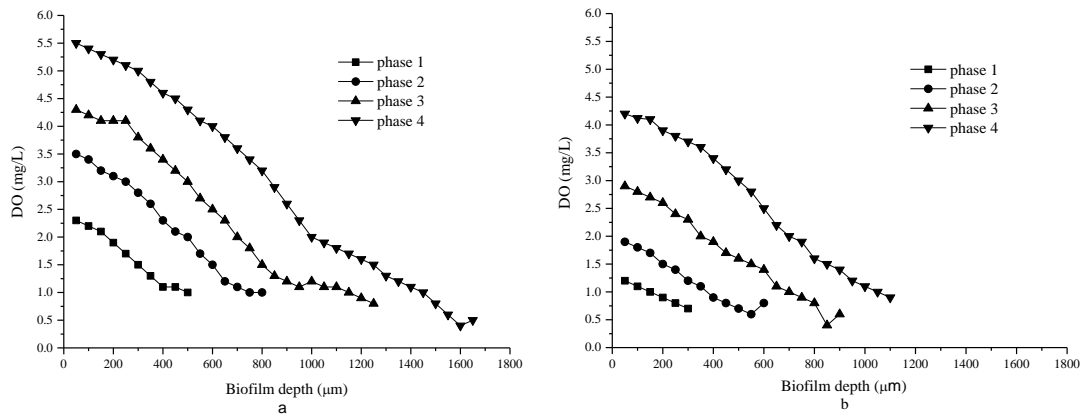


Fig. 5 DO distribution in biofilms of the heterotrophic nitrification zone (left) and hydrogenotrophic denitrification zone (right) in four phases

At the end of the experiment (95 days, four phases), the concentrations of  $\text{NH}_4^+\text{-N}$ ,  $\text{NO}_3^-\text{-N}$ ,  $\text{NO}_2^-\text{-N}$ , TN and COD at different depths of the reactor were measured. As

show in Fig. 4,  $\text{NH}_4^+\text{-N}$  and COD abruptly decreased to the lowest value (close to zero) with depth. However,  $\text{NO}_3^-\text{-N}$  increased gradually in the heterotrophic nitrification zone (nitrification dominated the nitrogen removal process), then decreased in the hydrogenotrophic denitrification section (denitrification dominated the process); almost no  $\text{NO}_2^-\text{-N}$  accumulated in the whole process. In the heterotrophic nitrification zone, the concentration of  $\text{NH}_4^+\text{-N}$  decreased from 56  $\text{mg L}^{-1}$  to 2.1  $\text{mg L}^{-1}$  (Fig. 4) while both of  $\text{NO}_3^-\text{-N}$  and  $\text{NO}_2^-\text{-N}$  increased, which proved that nitrification occurred. Meanwhile, the TN removal rate (above 50%) during phase 4 in Fig. 2c illustrates that significant denitrification took place in this point. As for the hydrogenotrophic denitrification section,  $\text{NH}_4^+\text{-N}$  and COD decreased gradually with the reactor height, which showed partial nitrification could occur in this section.  $\text{NO}_2^-\text{-N}$  went up to 10.6  $\text{mg L}^{-1}$  firstly and then reduced to 2.1  $\text{mg L}^{-1}$  (Fig. 4), moreover, there was similar variation trend in  $\text{NO}_3^-\text{-N}$ . This suggests both nitrification and denitrification could occur in the upper denitrification zone. These phenomena confirmed simultaneous nitrification and denitrification had been achieved in the different parts of the reactor.

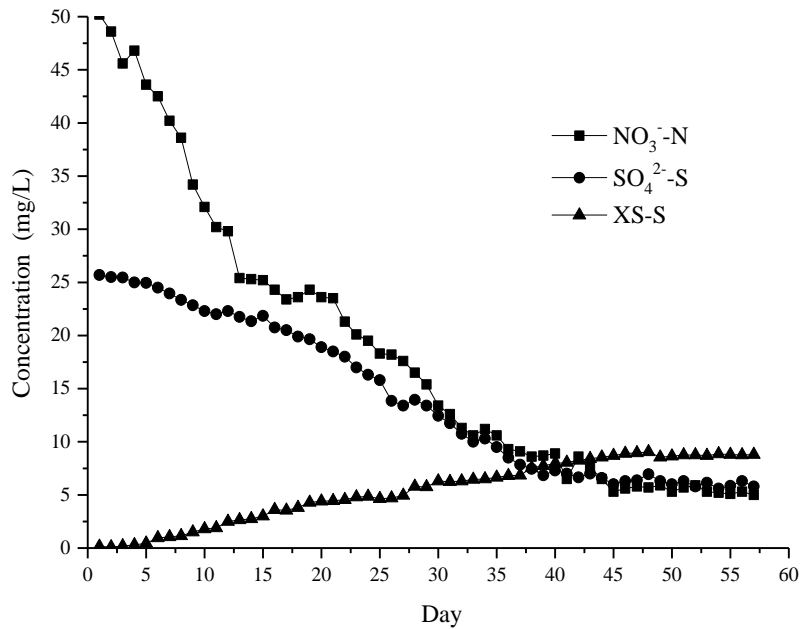
The transfer and consumption of DO in the biofilm serve important functions in nitrogen removal in the UBER system. Excessively high DO transfer resistance in the biofilm results in the aerobic layer being too thin and complicates ammonia oxidation. Conversely, excessively low DO transfer resistance makes the anaerobic layer too thin and slows down denitrification [28-29]. Determining the DO content in the biofilm is

297 helpful for understanding the mechanism of nitrogen removal. The DO  
298 microdistributions (by microelectrode) in the nitrification and denitrification biofilms  
299 are shown in Fig. 5. In the heterotrophic nitrification zone, the thickness of biofilm at  
300 phase 1 was 500  $\mu\text{m}$  and then increased with time. Consequently, the thickness of  
301 biofilm increased to 1650  $\mu\text{m}$  during phase 4. There was a similar pattern in the  
302 hydrogenotrophic denitrification zone, where the thickest biofilm was 1100  $\mu\text{m}$  at  
303 phase 4. The thickness of both biofilms increased with time, showing a continued  
304 growth of the microbial communities. It also can be seen that biofilm thicknesses in  
305 the heterotrophic nitrification section were thicker than those in the hydrogenotrophic  
306 denitrification section at the same phase. This result was in accordance with the fact  
307 that heterotrophic microorganisms have faster growth rates than autotrophic  
308 microbes. For the DO microdistribution in biofilms in the heterotrophic nitrification  
309 zone (Fig. 5, left), the DO levels in the biofilm declined to approximately 1.1  $\text{mg L}^{-1}$   
310 and then maintained a similar level, though the bulk DO values were different in  
311 different phases. Similar trends were shown in the hydrogenotrophic denitrification  
312 zone (Fig. 5, right), where the DO levels in the biofilms continuously dropped to  
313 nearly 0.5  $\text{mg L}^{-1}$ . The maximum DO in the upper and lower parts were 4.2  $\text{mg L}^{-1}$   
314 and 5.5  $\text{mg L}^{-1}$ , respectively. DO in biofilms decreased with the depth of biofilms at  
315 all phases. Thus, nitrification occurred in the outer layer of the biofilms consumed  
316 oxygen, which contributed to low DO conditions inside for anoxic denitrification. The  
317 DO variation in the biofilms indicated that nitrification can occur in the outer layer of

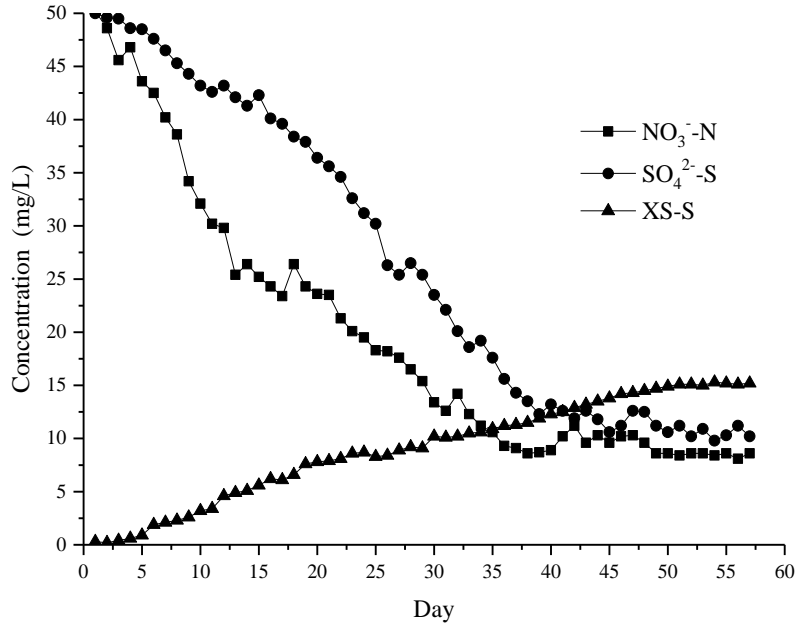
the biofilms whereas denitrification can occur in the inner layer.

Overall, nitrification and denitrification for nitrogen removal with the UBER system could be realized simultaneously. Simultaneous nitrification and denitrification was not only achieved through the whole reactor but also in the individual heterotrophic nitrification zone and hydrogenotrophic denitrification zone, respectively.

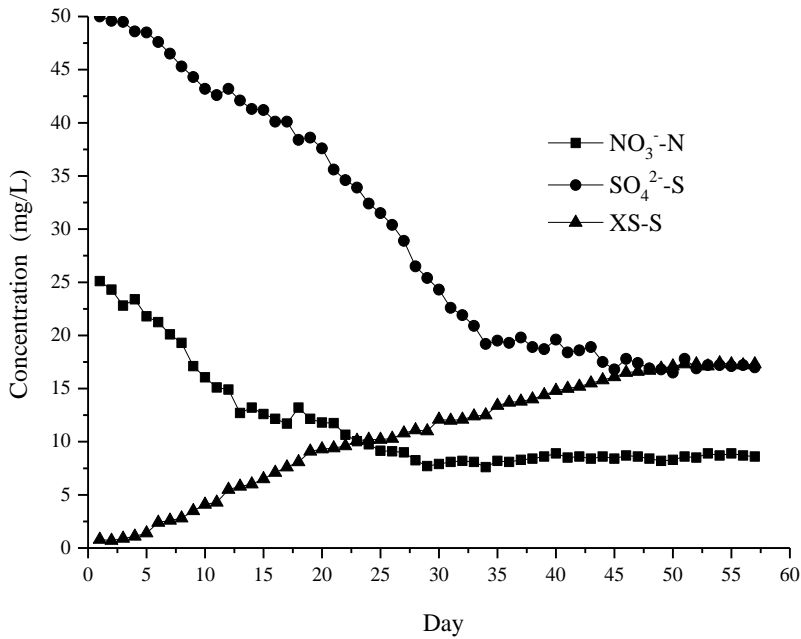
### 3.4. Effect of sulfate on hydrogenotrophic denitrification



(a)



(b)



(c)

Fig. 6 The concentrations of substrate in the effluents of the reactor at different S/N ratio (a)S/N=1:2; (b)S/N=1:1; (c)S/N=2:1 (XS-S refers to sulfide)

As shown in Fig. 6a, when the S/N ratio was 1:2, both effluent  $\text{NO}_3^- \text{-N}$  and  $\text{SO}_4^{2-} \text{-S}$  decreased to  $\sim 5 \text{ mg L}^{-1}$ , the concentration of XS-S gradually increased to  $\sim 8$

335  $\text{mg L}^{-1}$ . The average removal rate of  $\text{NO}_3^- \text{-N}$  ( $1 \text{ mg (L d)}^{-1}$ ) was significantly greater  
 336 than that of  $\text{SO}_4^{2-} \text{-S}$  ( $0.44 \text{ mg (L d)}^{-1}$ ) when the effluent parameters remained stable.  
 337 The concentration of  $\text{NO}_3^- \text{-N}$  and  $\text{SO}_4^{2-} \text{-S}$  kept declining when the XS-S reached  
 338 about  $8 \text{ mg L}^{-1}$ . Finally, the removal rates of  $\text{NO}_3^- \text{-N}$  and  $\text{SO}_4^{2-} \text{-S}$  reached  $\sim 80\%$ . The  
 339 results indicate that effective removal of nitrate and sulfate can be achieved  
 340 simultaneously at low S/N ratio since this concentration of XS-S ( $8 \text{ mg L}^{-1}$ ) didn't  
 341 inhibit hydrogenotrophic denitrification. Under a 1:1 S/N ratio, effluent  $\text{SO}_4^{2-} \text{-S}$   
 342 dropped to  $\sim 10 \text{ mg L}^{-1}$  and XS-S went up to  $15 \text{ mg L}^{-1}$ . When the effluent  
 343 concentration of  $\text{NO}_3^- \text{-N}$  was higher than  $15 \text{ mg L}^{-1}$  (the first 13 days), the removal  
 344 rate of  $\text{NO}_3^- \text{-N}$  ( $1.9 \text{ mg (L d)}^{-1}$ ) was greater than that of  $\text{SO}_4^{2-} \text{-S}$  ( $0.54 \text{ mg (L d)}^{-1}$ ). The  
 345 effluent concentration of  $\text{NO}_3^- \text{-N}$  remained stable ( $7 \text{ mg L}^{-1}$ ) after 37 days, while the  
 346 XS-S was  $10 \text{ mg L}^{-1}$ . At that stage, the average removal rate of  $\text{SO}_4^{2-} \text{-S}$  was equal to  
 347  $\text{NO}_3^- \text{-N}$  ( $1.25 \text{ mg (L d)}^{-1}$ ). After 50 days, the XS-S increased to  $15 \text{ mg L}^{-1}$  and the  
 348  $\text{SO}_4^{2-} \text{-S}$  reached a stable level ( $10 \text{ mg L}^{-1}$ ) (Fig. 6b). It can be inferred that the  
 349 denitrification process was inhibited when the XS-S reached  $10 \text{ mg L}^{-1}$ , and sulfate  
 350 reduction was inhibited when it reached  $15 \text{ mg L}^{-1}$ .

351 Results were similar with a S/N ratio of 2:1 (Fig. 6c). After 28 days, the  
 352 concentration of XS-S reached  $10 \text{ mg L}^{-1}$  and effluent  $\text{NO}_3^- \text{-N}$  was stable at about  $7$   
 353  $\text{mg L}^{-1}$ . The average removal rate of  $\text{NO}_3^- \text{-N}$  was similar to  $\text{SO}_4^{2-} \text{-S}$  ( $0.7 \text{ mg (L d)}^{-1}$ ).  
 354 When the XS-S increased to  $15 \text{ mg L}^{-1}$  at day 45, the  $\text{SO}_4^{2-} \text{-S}$  equilibrium  
 355 concentration ( $15 \text{ mg L}^{-1}$ ) was achieved. Denitrification and sulfate reduction

processes were inhibited when the XS-S reached 10 mg L<sup>-1</sup> (day 28) and 15 mg L<sup>-1</sup> (day 45), respectively. The final removal rates of NO<sub>3</sub><sup>-</sup>-N and SO<sub>4</sub><sup>2-</sup>-S were below 68%. In the three groups of experiments, the denitrification percent declined and time for stable effluent NO<sub>3</sub><sup>-</sup>-N shortened as S/N ratio increased. Further studies are needed on how sulfate inhibits hydrogenotrophic denitrification: competition for electronic donors or the toxicity of sulfide on denitrifying bacteria.

#### **4. Conclusions**

The SND could be achieved with the novel UBER system for synthetic wastewater treatment. DO in bulk solution was an important factor that affected the nitrification and denitrification processes in both heterotrophic nitrification and hydrogenotrophic denitrification sections of the reactor. The experimental results indicated that high nitrogen removal efficiency could be achieved through SND by the UBER system. Relatively high DO concentration didn't inhibit hydrogen autotrophic denitrification significantly. Simultaneous removal of NO<sub>3</sub><sup>-</sup>-N and SO<sub>4</sub><sup>2-</sup>-S can be achieved at low S/N ratio, but higher ratios caused inhibition of denitrification and sulfate reduction

#### **Acknowledgements**

This work was conducted with financial support from the Strategic Priority Research Program of the Chinese Academy of Sciences (Grant No.:XDA23050203) and the National Natural Science Foundation of China (Grant No: 41373100).

Additional supports were provided by the CAS Key Technology Talent Program.

## References

- [1] Y. Xiao, S. Wu, Z. H. Yang, Z. J. Wang, C. Z. Yan and F. Zhao, In situ probing the effect of potentials on the microenvironment of heterotrophic denitrification biofilm with microelectrodes, *Chemosphere.*, 93(2013), 1295-1300.
- [2] F. Rezvani, M. H. Sarrafzadeh, S. Ebrahimi and H. M. Oh, Nitrate removal from drinking water with a focus on biological methods: a review, *Environ. Sci. Pollut. Res.*, 16(2017), 1-18.
- [3] S. K. Gupta, S. M. Raja and A. B. Gupta, Simultaneous nitrification-denitrification in a rotating biological contactor, *Environ. Technol.*, 15(1994), 145-153.
- [4] S. B. He, G. Xue and B. Z. Wang, Factors affecting simultaneous nitrification and denitrification (SND) and its kinetics model in membrane bioreactor, *J. Hazard. Mater.*, 168(2009), 704-710.
- [5] J. Guo, L. Zhang, W. Chen, F. Ma, H. Liu and Y. Tian, The regulation and control strategies of a sequencing batch reactor for simultaneous nitrification and denitrification at different temperatures, *Bioresour. Technol.*, 133(2013), 59-67.
- [6] I. J. Kugelman, M. Spector, A. Harvilla and D. Paress, Aerobic denitrification in activated-sludge, *Environ. Eng.*, 4(1991), 312-318.
- [7] M. Morita, H. Uemoto and A. Watanabe, Nitrogen-removal bioreactor capable of simultaneous nitrification and denitrification for application to industrial wastewater treatment, *Biochem. Eng. J.*, 41(2008), 59-66.
- [8] M. Seifi and M. H. Fazelipour, Modeling simultaneous nitrification and denitrification (SND) in a fluidized bed biofilm reactor, *Appl. Math. Model.*, 36(2012), 5603-5613.
- [9] X. Wang, S. Wang, J. Zhao, X. Dai and Y. Peng, Combining simultaneous nitrification-endogenous denitrification and phosphorus removal with post-denitrification for low carbon/nitrogen wastewater treatment, *Bioresour. Technol.*, 220(2016), 17-25.
- [10] L. Yan, S. Zhang, G. Hao, X. Zhang, Y. Ren, Y. Wen, Y. Guo and Y. Zhang, Simultaneous nitrification and denitrification by EPSs in aerobic granular sludge enhanced nitrogen removal of ammonium-nitrogen-rich wastewater, *Bioresour. Technol.*, 202(2016), 101-106.
- [11] L. A. Robertson, R. Cornelisse, V. P. De, R. Hadjoetomo and J. G. Kuenen, Aerobic denitrification in various heterotrophic nitrifiers, *Antonie Van Leeuwenhoek.*, 56(1989), 289-299.
- [12] Y. Sakakibara and M. Kuroda, Electric prompting and control of denitrification, *Biotechnol. Bioeng.*, 42(1993), 535-537.
- [13] S. Ghafari, M. Hasan and M. K. Aroua, Nitrate remediation in a novel up flow bio-electrochemical reactor (UBER) using palm shell activated carbon as cathode



- material, *Electrochim. Acta.*, 54(2009), 4164-4171.
- [14] A. Chidthaisong and R. Conrad, Turnover of glucose and acetate coupled to reduction of nitrate, ferric iron and sulfate and to methanogenesis in anoxic rice field soil, *FEMS Microbiol. Ecol.*, 31(2000), 73–86.
- [15] C. Chen, X. J. Xu, P. Xie, Y. Yuan, X. Zhou, A. J. Wang, D. J. Lee and N. Q. Ren, Pyrosequencing reveals microbial community dynamics in integrated simultaneous desulfurization and denitrification process at different influent nitrate concentrations, *Chemosphere.*, 171(2016), 294.
- [16] M. Zheng, Y. Q. Sheng, R. C. Sun, C. G. Tian, H. B. Zhang, J. C. Ning, Q. R. Sun, Z. R. Li, S. H. Bottrell and R. G. Mortimer, Identification and quantification of nitrogen in a reservoir, Jiaodong Peninsula, China, *Water Environ. Res.*, 89(2017), 369-377.
- [17] American Public Health Association/American Water Works Association/Water Environment Federation, *Standard Methods for the Examination of Water and Wastewater* 20th edn, Washington DC, USA, 1998.
- [18] W. De Boer and G. A. Kowalchuk, Nitrification in acid soils: micro-organisms and mechanisms, *Soil Biol. Biochem.*, 33(2001), 853-866.
- [19] J. Zhang, W. Sun, W. Zhong and Z. Cai, The substrate is an important factor in controlling the significance of heterotrophic nitrification in acidic forest soils, *Soil Biol. Biochem.*, 76(2014), 143-148.
- [20] A. E. Amoo and O. O. Babalola, Ammonia-oxidizing microorganisms: key players in the promotion of plant growth, *J. Soil Sci. Plant Nutr.*, 17(2017), 935-947.
- [21] H. J. Hamlin, J. T. Michaels, C. M. Beaulaton, W. F. Grahama, W. Dutta P. Steinbachb, T. M. Losordoc, K. K. Schraderd and K. L. Maina, Comparing denitrification rates and carbon sources in commercial scale upflow denitrification biological filters in aquaculture, *Aquacultural Engineering*, 38(2008), 79-92.
- [22] Z. Q. Shen, Y. X. Zhou and J. L. Wang, Comparison of denitrification performance and microbial diversity using starch/polylactic acid blends and ethanol as electron donor for nitrate removal, *Bioresour. Technol.*, 131(2013), 33-39.
- [23] N. Sunger and P. Bose, Autotrophic denitrification using hydrogen generated from metallic iron corrosion, *Bioresour. Technol.*, 100(2009), 4077-82.
- [24] H. I. Park, S. K. Ji, K. K. Dong, Y. J. Choi and D. Pak, Nitrate-reducing bacterial community in a biofilm-electrode reactor, *Enzyme Microb. Technol.*, 39(2006), 453-458.
- [25] S. H. Deng, D. S. Li, X. Yang, S. B. Zhu and J. L. Li, Process of nitrogen transformation and microbial community structure in the Fe(0)-carbon-based bio-carrier filled in biological aerated filter, *Environ. Sci. Pollut. Res.*, 23(2016), 6621-6630.
- [26] P. Li, W. Xing, J. N. Zuo, L. Tang, Y. J. Wang and J. Lin, Hydrogenotrophic

- denitrification for tertiary nitrogen removal from municipal wastewater using  
membrane diffusion packed-bed bioreactor, *Bioresour. Technol.*, 144(2013),  
452-459.
- [27] J. C. Alzate Marin, A. H. Caravelli and N. E. Zaritzky, Nitrification and aerobic  
denitrification in anoxic-aerobic sequencing batch reactor, *Bioresour. Technol.*,  
200(2015), 380-387.
- [28] Y. F. Ning, Y. P. Chen, Y. Shen, N. Zeng, S. Y. Liu, J. S. Guo and F. Fang, A new  
approach for estimating aerobic-anaerobic biofilm structure in wastewater  
treatment via dissolved oxygen microdistribution, *Chem. Eng. J.*, 255(2014),  
171-177.
- [29] X. Wen, J. Zhou, J. L. Wang, X. X. Qing and Q. He, Effects of dissolved oxygen  
on microbial community of single-stage autotrophic nitrogen removal system  
treating simulating mature landfill leachate, *Bioresour. Technol.*, 218(2016),  
962-968.